

Effects of aggregation on the excitation transfer in perylene-end-capped polyindenofluorene studied by time-resolved photoluminescence spectroscopy

L. M. Herz, C. Silva, R. H. Friend, and R. T. Phillips
Cavendish Laboratory, Madingley Road, Cambridge, CB3 0HE, United Kingdom

S. Setayesh, S. Becker, D. Marsitsky, and K. Müllen
Max-Planck-Institut für Polymerforschung, Ackermannweg 10, D-55128 Mainz, Germany

(Received 1 December 2000; revised manuscript received 2 March 2001; published 17 October 2001)

We have investigated the excitation transfer in a system comprising poly(6,6',12,12'-tetra-2-ethylhexyl-2,8-indenofluorene) (PIFTEH) chains end-capped with perylene dye molecules, using femtosecond time-resolved photoluminescence (PL) spectroscopy as well as polarized photoluminescence measurements. The transfer of excitons from isolated PIFTEH chains to perylene molecules is completed within the first 30–40 ps after excitation, and we extract a Förster radius $R_0 = (1.8 \pm 0.3)$ nm from the time-resolved PL transients. We have modelled the polarization anisotropy for a guest-host system subject to Förster interactions via a Monte Carlo simulation and find that the emission from acceptors becomes unpolarized at sufficiently large acceptor concentrations, permitting an accurate determination of the Förster radius from time-integrated photoluminescence anisotropy measurements. While spectral overlap calculations predict a large efficiency for the transfer of excitations to the perylene molecules from sites where the PIFTEH chains aggregate, no transfer is observed experimentally, which we attribute to chain packing effects within the sample prohibiting sufficiently close contact between PIFTEH aggregates and perylene molecules.

DOI: 10.1103/PhysRevB.64.195203

PACS number(s): 78.47.+p, 78.66.Qn, 78.55.-m

I. INTRODUCTION

The ease of production of bright, efficient polymer light emitting diodes (LED's) has stimulated intensive research into the photophysical properties of luminescent conjugated polymers within the last decade.¹ More recently, attention has been focussed onto polymer-based guest-host systems, in which even at low guest concentration the luminescence is dominated by the guest due to efficient transfer of excitation from the host.^{2–6} Advantages of such systems include lower thresholds for amplified spontaneous emission as a result of reduced self-absorption,^{7,8} as well as improved electroluminescence efficiencies caused by confinement of positively and negatively charged carriers within guest regions.^{9,10} Moreover, guest-host systems offer colortunability through changes in either the type, or the concentration of the guest thereby permitting the simplified production of color displays based on a common host polymer.^{10,11} Excitation transfer has also been exploited for the design of polarizing filters, where light is absorbed by an isotropic host and transferred to an oriented guest,^{12,13} and has been used to increase the efficiency of solar cells by expanding the effective absorption range.¹⁴ Systems investigated so far have mainly consisted of polymer-polymer blends^{3,6,7,9} or polymeric hosts doped with dye molecules as guests.^{15,2,12} In this paper we will give a detailed account of the Förster transfer in a novel polymer α,ω -Bis(N-(2,6-diisopropylphenyl)-1,6-bis(4-*t*-butylphenoxy)-3,4-dicarbonyl acidimide-9-perylenepoly-2,8-(6,6,12,12-tetraethylhexyl)indenofluorene (PEC-PIFTEH), which has perylene derivatives bonded covalently to both ends of a polyindenofluorene chain [Fig. 1(a)]. We will show that the morphology within the sample has a significant influence on the efficiency of the excitation transfer: while the majority of excitations created on isolated polymer chains is transferred

to the perylene end-caps, hardly any transfer occurs from sites where polymer chains aggregate, as the contact between the polymeric hosts and the perylene guests is insufficient at these locations.

II. SAMPLE PREPARATION AND EXPERIMENTAL TECHNIQUE

The general synthesis of conjugated polymers covalently coupled to perylene derivatives is described elsewhere.¹⁶ Thin films were produced of either PEC-PIFTEH or the PIFTEH homopolymer by spin casting from anhydrous *p*-xylene solutions on Spectrosil substrates, which resulted in film thicknesses of ≈ 100 nm. Films were prepared, stored and mounted in a glovebox and were kept at 10^{-6} mbar during the experiments to avoid photo-oxidation. To estimate the molar extinction coefficient spectrum of the perylene derivative in PEC-PIFTEH, a polymer consisting of closely related perylene momomers was dissolved in chloroform at various concentrations.

To study the time-dependent energy transfer in PEC-PIFTEH films we have performed time-resolved photoluminescence (PL) experiments on both PEC-PIFTEH and PIFTEH homopolymer films, by using the up conversion technique. The sample was excited with the frequency-doubled output from a mode-locked Ti:sapphire laser supplying 120-fs pulses at an energy of 3.1 eV at a repetition rate of 82 MHz. Photoluminescence originating from the sample was collected with dispersion-free optics and up converted in a β -barium-borate (BBO) crystal using the fundamental laser beam at 1.55 eV as a gate. Sum-frequency photons were dispersed in a monochromator and detected using a UV-enhanced, nitrogen cooled Si-CCD detector. Zero delay was set to the peak of the cross-correlation between the light

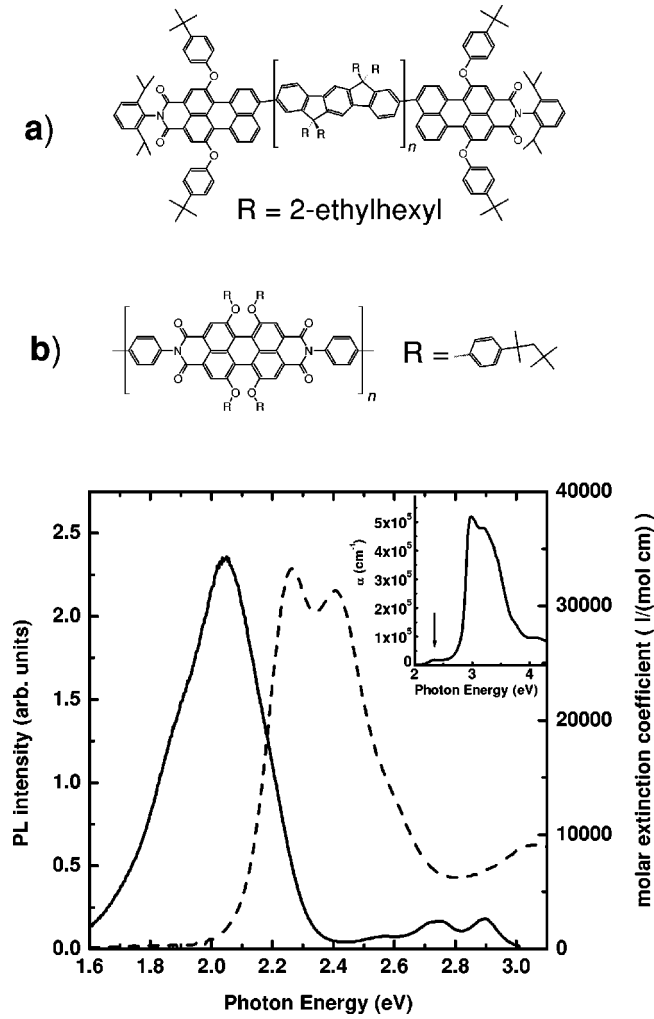


FIG. 1. Top: (a) Chemical structure of PEC-PIFTEH. (b) Chemical structure of the polyperylene derivative. Bottom: Photoluminescence spectrum of a PEC-PIFTEH film (solid line) together with the molar extinction coefficient ϵ_A of the polyperylene derivative in chloroform solution (dashed line). The inset shows the absorption spectrum of a PEC-PIFTEH film, where the arrow indicates the maximum of the absorption due to perylene molecules.

scattered from the sample surface and the gate beam in the BBO crystal. The overall temporal resolution is given by the full width at half maximum of the cross correlation to be 280 fs. The average excitation power on the sample was 0.82 mW on a spot of $\approx 110 \mu\text{m}$ diameter. To measure time-integrated PL, the BBO crystal was replaced by a linear polarizer and the UV-pass filter (Schott UG11) in front of the spectrometer was removed. To vary the detection polarization with respect to the excitation polarization, the latter was adjusted by rotation of a $\lambda/2$ -plate and a Glan-Thompson polarizing prism. Both time-resolved and time-integrated spectra were corrected for spectral response. All experiments were performed at room temperature.

III. RESULTS AND DISCUSSION

Figure 1(a) shows the chemical structure of PEC-PIFTEH, which consists of a polyindeno[1,2,3-cd]fluorene chain with

2-ethylhexyl side chains (PIFTEH), terminated on each end by a perylene dye molecule. The polyindeno[1,2,3-cd]fluorene chain lengths range between 13–29 repeat units with an effective conjugation length of approximately 6 repeat units.¹⁷ Since the relative concentration of the perylene molecules is low ($\approx 5.5\%$ by mole fraction), light at a photon energy of 3.1 eV will create excitations almost exclusively on the PIFTEH chains. However, as can be seen in Fig. 1, the photoluminescence from PEC-PIFTEH is dominated by the emission from the perylene molecules ($\approx 1.7\text{--}2.3$ eV), while only a small fraction of it originates from recombination of excitations located on the PIFTEH main chains ($\approx 2.4\text{--}3.0$ eV). This indicates an efficient energy transfer between the PIFTEH main chains and the perylene end caps. Due to the large spectral overlap between the PIFTEH emission and the perylene absorption (see Fig. 1), Förster interaction is expected to give a major contribution to the transfer of excitation.¹⁸

Förster's theory was originally developed to describe the phenomenon of luminescence depolarization with increasing concentration of luminescent molecules in viscous solutions.^{19–22} It predicts a transfer rate $K_{D \rightarrow A}$ between a donor-acceptor pair, which is inversely proportional to the sixth power of the separation R between a donor and an acceptor, that is¹⁸

$$K_{D \rightarrow A} = \frac{1}{\tau_D} \left(\frac{R_0}{R} \right)^6, \quad (1)$$

where

$$R_0 = \left[\frac{9000 \ln 10}{128 \pi^5} \frac{\kappa^2 \eta_D}{n^4 N} \int_0^\infty f_D(\bar{\nu}) \epsilon_A(\bar{\nu}) \frac{d\nu}{\bar{\nu}^4} \right]^{1/6} \quad (2)$$

is the ‘‘Förster radius,’’^{23–28} or the donor-acceptor separation at which excitation transfer from a donor is as likely to occur as de-excitation by all other means. Here, η_D is the luminescence efficiency of the donor in the absence of acceptors, n is the refractive index of the material (at the peak of the integrand), $N = 6.022 \times 10^{23}$ is Avogadro's constant, $\epsilon_A(\bar{\nu})$ is the molar decadic extinction coefficient of the acceptor (entered in units of $1 \text{ mol}^{-1} \text{ cm}^{-1}$), f_D is the fraction of photons with wave number $\bar{\nu}$ emitted per unit wave number from the donor in the absence of absorbers, and κ^2 is a factor related to the orientation of the donor and the acceptor dipole moments \vec{d} , \vec{a} , as well as the direction \vec{r} between the origin of the donor and the origin of the acceptor²⁶

$$\kappa^2 = [\vec{d} \cdot \vec{a} - 3(\vec{d} \cdot \vec{r})(\vec{a} \cdot \vec{r})]^2, \quad (3)$$

where $|\vec{d}| = |\vec{a}| = |\vec{r}| = 1$. In solutions of low viscosity, where Brownian rotation of the donor and the acceptor is sufficiently fast, an average value of $\kappa^2 = 2/3$ may be used.^{26,29} However, this is not the case in solid polymer films where the dipole moments have fixed orientations during the time scale of the transfer. An average over a donor-acceptor ensemble with random but fixed orientations³⁰ yields $\kappa^2 = (0.845\sqrt{2/3})^2$ and is then a more appropriate choice. Equation (1) describes the transfer rate for a *single* donor-acceptor

pair; for a given spatial distribution of donors and acceptors, an ensemble average over all possible transfers needs to be taken. If a random spatial distribution of donors and acceptors is assumed, one obtains³¹

$$K_{D \rightarrow A} = \frac{\beta}{\sqrt{t}} \quad (4)$$

with

$$\beta = \frac{1}{2} \sqrt{\pi} \frac{c_A}{c_0} \frac{1}{\sqrt{\tau_D}} \quad \text{and} \quad c_0 = \left(\frac{4\pi}{3} R_0^3 \right)^{-1}, \quad (5)$$

where c_A is the acceptor concentration and c_0 is the ‘‘critical concentration.’’³² The time-dependence of $K_{D \rightarrow A}$ originates from the fact that the originally random distribution of excited donors and acceptors becomes less random with time, as donors located close to acceptors transfer their excitation faster than those located further away. The transfer efficiency thus decreases with increasing time after the excitation.²⁸ Using Eq. (4) the Förster transfer within a randomly distributed ensemble can be described by the following set of rate equations^{32,33,28}

$$\frac{d}{dt} n_D = G(t) - \frac{n_D}{\tau_D} - \frac{\beta}{\sqrt{t}} n_D, \quad (6)$$

$$\frac{d}{dt} n_A = \frac{\beta}{\sqrt{t}} n_D - \frac{n_A}{\tau_A},$$

where n_D (n_A) is the number of excited donors (acceptors), τ_D (τ_A) is the recombination rate of the donors (acceptors) in the absence of the acceptors (donors), and $G(t)$ is the rate at which excited donors are created. Equations (6) only apply to the low-density regime, where interactions between the excitations can be neglected. For $G(t) = N_D \delta(t)$ the solutions are given by

$$n_D = N_D \exp\left(-\frac{t}{\tau_D} - 2\beta\sqrt{t}\right), \quad (7)$$

$$n_A = N_A \left[\psi\left(\frac{\beta}{\alpha} + \alpha\sqrt{t}\right) - \psi\left(\frac{\beta}{\alpha}\right) \right] \exp\left(-\frac{t}{\tau_A}\right),$$

where $\psi(x) = (2/\sqrt{\pi}) \int_0^x e^{-y^2} dy$ is the error function, $\alpha = \sqrt{\tau_D^{-1} - \tau_A^{-1}}$ and $N_A = N_D \sqrt{\pi} \beta / \alpha e^{\beta^2/\alpha^2}$. Integration of Eq. (7) over time yields the total transfer probability φ_T from the donor to the acceptor ensemble, as well as the fraction ϕ_D (ϕ_A) of photons emitted from the donors (acceptors):

$$\varphi_T(X) = \sqrt{\pi} X e^{X^2} [1 - \psi(X)], \quad (8)$$

$$\phi_D = \eta_D (1 - \varphi_T), \quad \text{and} \quad \phi_A = \eta_A \varphi_T$$

where $X = \beta \sqrt{\tau_D} = \frac{1}{2} \sqrt{\pi} (c_A/c_0)$ and η_D (η_A) is the radiative efficiency of the donors (acceptors) in the absence of acceptors (donors). Equations (1)–(8) provide three possible means to assess the strength of the Förster interaction in a system from experimental data: The Förster radius R_0 can be

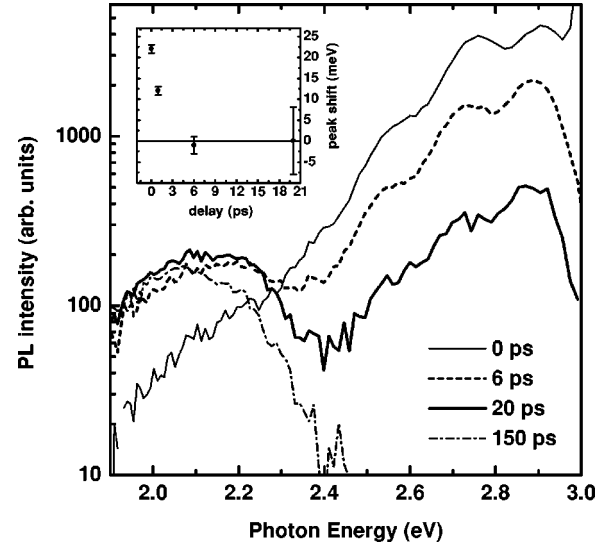


FIG. 2. Time-resolved photoluminescence spectra for PEC-PIFTEH at various times after excitation. The insert shows the peak energy shift of the 0-0 vibronic transition with time after excitation.

extracted from comparison of Eq. (7) to the time-resolved photoluminescence originating from the donors and the acceptors. It may also be calculated using Eq. (8) from the ratio ϕ_D/ϕ_A of photons emitted from donors, to photons emitted from acceptors, which can be taken from the time-integrated PL spectra. Finally, one may obtain R_0 from Eq. (2) by determining the spectral overlap between the donor emission and the acceptor absorption.

Figure 2 displays the time-resolved photoluminescence spectra for PEC-PIFTEH within the first 150 ps after excitation. Within the spectral region of the emission from the PIFTEH main chains (2.4–3.0 eV) a fast decay of the photoluminescence is observed, which is accompanied by a corresponding rise in the red luminescence from perylene molecules (1.9–2.4 eV). The energy transfer from the PIFTEH main chains to the perylene molecules is almost completed within the first 30 ps after excitation. However, a closer look at the emission from the sample at 0 ps delay reveals a broad red tail in the photoluminescence between 1.9 and 2.4 eV, which is present even before any significant amount of transfer could have occurred. We therefore attribute this tail to the emission from excitations located on those PIFTEH main chains subject to interchain interactions. Redshifted luminescence bands have been observed for materials similar to PIFTEH, such as poly-9,9-dioctylfluorene (PFO) for which they were shown to appear within less than 400 fs after excitation,³⁴ and for poly-2,8-indenofluorene with octyl side chains (PIFTO).³⁵ We have also found the signature of these long-lived emission bands in the time-resolved photoluminescence from films consisting of the PIFTEH homopolymer, although at a much smaller extent when compared with PIFTO films.³⁶ While it was shown that interchain interactions in polyfluorene films result in the formation of excimers,³⁷ we have no evidence clarifying whether this is also the case in PIFTEH. We will from now on refer to these species as ‘‘aggregates’’ regardless of whether they exist in their ground state or only in their excited state.³⁸ The exist-

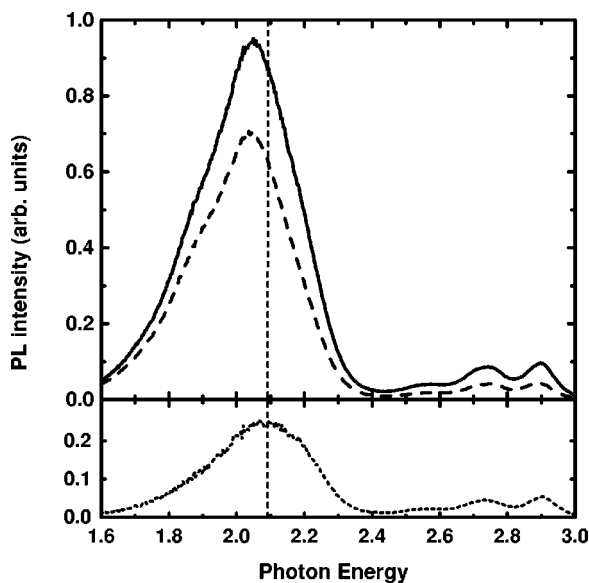


FIG. 3. Top: Time-integrated photoluminescence spectra from a PEC-PIFTEH film with the luminescence polarization set either parallel (solid line) or perpendicular (dashed line) to the excitation polarization direction. Bottom: Difference spectrum $I_{\parallel} - I_{\perp}$; the dashed vertical line indicates the peak of the emission from PIFTEH aggregates.

tence of emission from PIFTEH aggregates within the PEC-PIFTEH film is confirmed by our measurements of the time-integrated photoluminescence anisotropy: Fig. 3 shows the time-integrated photoluminescence spectrum from PEC-PIFTEH with polarization either parallel (I_{\parallel}) or perpendicular (I_{\perp}) to the excitation polarization direction. Because linearly polarized light will preferentially excite PIFTEH chains oriented parallel to the polarization direction, a certain degree of polarization can be expected for the emission from the PIFTEH chains and is indeed observed. However, even though the Förster transfer probability contains a dependence on the relative orientation of the donor-acceptor pair through the orientation factor κ^2 , it is generally assumed that Förster transfer results in an almost randomly oriented ensemble of excited acceptors emitting unpolarized light.^{39,40} This assumption is supported by our model simulations which we will describe later. The fact that we find a considerable polarization anisotropy at the low energy side of the PL spectrum therefore indicates that part of the emission in the red still originates from the main PIFTEH chains. Since the luminescence from the perylene molecules should be unpolarized, the difference spectrum $I_{\parallel} - I_{\perp}$ will contain only the contribution from the PIFTEH main chains. As can be seen in Fig. 3 (bottom), the difference spectrum displays a broad, featureless luminescence peak in the red (centered at ≈ 2.1 eV), characteristic of the emission from aggregates in polymer films.^{41,42,37} The existence of PIFTEH-aggregates within the PEC-PIFTEH film needs to be taken into account for a correct description of the Förster transfer within the film.

To extract the Förster radius from the time-evolution of the donor and the acceptor excitation densities we have taken photoluminescence decay curves both in the spectral region

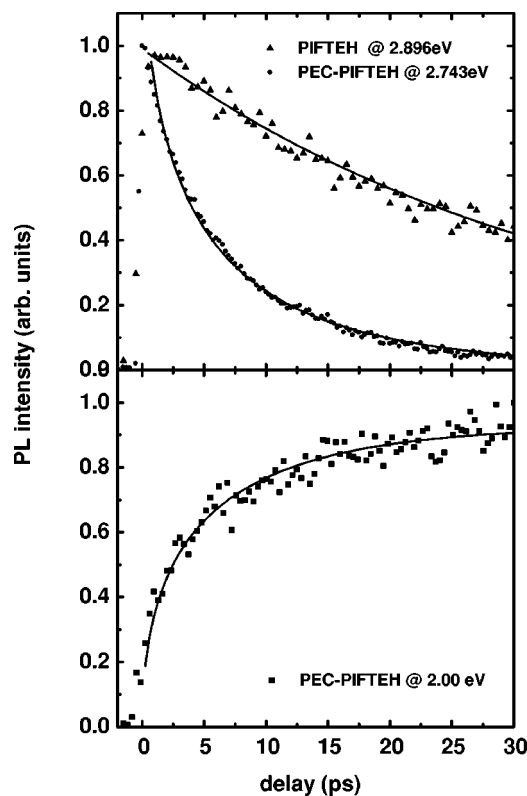


FIG. 4. Top: Photoluminescence decay in the excitonic emission region for a PEC-PIFTEH film (circles) as well as a film of the PIFTEH homopolymer (triangles). Bottom: Photoluminescence rise in the region of the perylene emission for a PEC-PIFTEH film (squares). Solid lines are fits to the data as described in the text.

of the PIFTEH main chain emission (2.743 eV) and in the region of the perylene luminescence (1.9–2.2 eV) as shown in Fig. 4. To determine the lifetime τ_D of the excitation on the PIFTEH chain in the absence of perylene molecules, we have also performed time-resolved photoluminescence measurements on films of the PIFTEH homopolymer. The excitonic emission from the PIFTEH homopolymer at 2.896 eV photon energy is found to have a monoexponential decay with $\tau_D = (35 \pm 2)$ ps (see Fig. 4, top).

List *et al.*⁵ has calculated from their study of energy transfer between ladder-type poly(*para*-phenylene) and orange-light-emitting macromolecules (RS19), that exciton migration between donor sites has a major influence on the transfer probability from the donors to the acceptors. However, we find that exciton migration only plays a very minor role in the excitation transfer in our system: time-resolved differential transmission experiments in dilute PEC-PIFTEH solutions have shown that transfer of excitations created on the PIFTEH main chains to the perylene end caps is inefficient and takes hundreds of picoseconds to occur.⁴³ We were also able to monitor the extent of exciton migration between PIFTEH chain segments prior to transfer by measuring the shift of the peak energy at the 0-0 vibronic transition in the time-resolved photoluminescence spectra^{44,45} (see inset of Fig. 2). We find a relatively modest shift of ≈ 22 meV which occurs within the first 2–3 ps after excitation. However, exciton migration should only assist the Förster transfer

at later times after excitation, when the transfer efficiency from an ensemble of localized donors decreases because only those donors are still excited which are located far from acceptors. It will cause a redistribution of the excitations within the donor ensemble and thus increase the transfer efficiency. At early times after excitation, exciton migration should not have a major impact on the transfer efficiency, as the distribution of excited donors will still be essentially random. We conclude that exciton migration between the donors thus only has a minor effect on the energy transfer between donors and acceptors in our system and can be neglected. In addition, quantum chemical and molecular mechanics calculations have revealed that the interchain Förster transfer rate is expected to be larger than the on-chain transfer rate by a few orders of magnitude.⁴³ Excitation transfer in our system therefore occurs predominantly between a donor located on one PIFTEH chain and an acceptor located on another chain nearby, with no correlation between the orientation of the donor's and the acceptor's dipole moments. The latter is supported by our observation of identical transfer dynamics for detection of the emission copolarized or cross polarized with the emission polarization (not shown).

We were able to obtain good fits to the photoluminescence transients using Eq. (7) with $\tau_D=35$ ps, $\tau_A=837$ ps and only β and a scaling constant as variable parameters (see Fig. 4). From the value of β extracted from the fits we then calculated R_0 from Eq. (5) taking $c_A=(0.7\pm 0.3)\times 10^{20}$ cm⁻³: We find $R_0=(1.8\pm 0.3)$ nm from the fits to the decay of the luminescence from the PIFTEH main chains and values varying between 2.0 and 1.4 nm for the fits to the PL rise in the low energy region between 1.9 and 2.2 eV. The variation of the latter values is due to the underlying aggregate emission and they are therefore less reliable than the value taken from the decay of the donor luminescence.

To evaluate the probability of Förster transfer between PIFTEH aggregates and perylene molecules we have taken photoluminescence decay curves in the spectral region between 2.2 and 2.3 eV where the luminescence is dominated by the emission from aggregate states. These curves are plotted in Fig. 5 together with monoexponential fits to the PL decay at long delays. We find PL decay times increasing from $\tau=232$ ps at 2.301 eV to 447 ps at 2.195 eV. These values are similar to those measured in PIFTEH and PIFTO homopolymer films,³⁶ indicating that while there is a *fast and efficient* transfer of excitons located on isolated PIFTEH chains to perylene molecules, the transfer of excitations from PIFTEH aggregates to perylene molecules is *substantially reduced*.

To obtain a measure of the Förster interactions in PEC-PIFTEH from the time-integrated photoluminescence spectra, the contribution from the aggregate emission to the red part of the spectrum needs to be estimated first. Figure 6 shows the emission anisotropy r for the PEC-PIFTEH film, calculated from I_{\parallel} and I_{\perp} as

$$r = \frac{I_{\parallel} - I_{\perp}}{I_{\parallel} + 2I_{\perp}}. \quad (9)$$

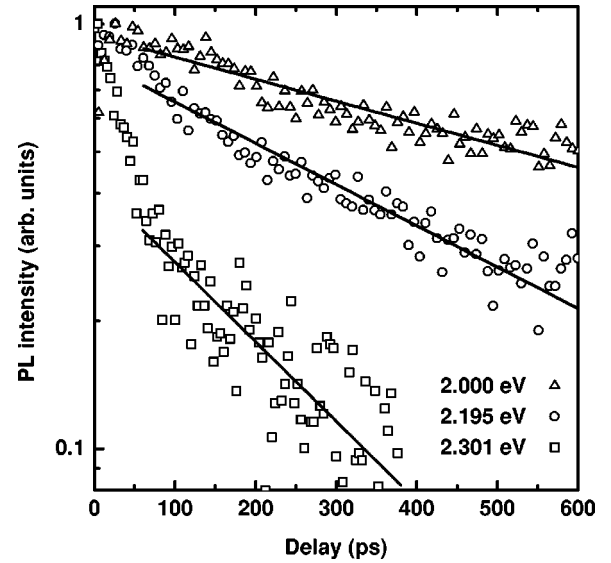


FIG. 5. Photoluminescence decay in the low-energy spectral region of the emission from PEC-PIFTEH, together with monoexponential fits to the data at long delays.

In the emission range of the PIFTEH main chains (2.4–3.0 eV) it is approximately constant ($r\approx 0.31$), but then decays to $r\approx 0.075$ at 1.6 eV. For a randomly oriented ensemble of absorbing and reemitting dipoles,⁴⁶ the emission anisotropy can assume a maximum value of $r_{\max}=0.4$ where processes such as excitation transfer or migration to other dipoles, as well as rotation of the original dipole, can reduce the emission anisotropy down to zero. We performed a Monte Carlo simulation to investigate whether the anisotropy in the distribution of excited PIFTEH main chains, caused by excitation with linearly polarized light, could at least partly be transferred to the perylene molecules within a Förster transfer, thereby causing an anisotropic emission from the perylene molecules. However, we find that only a vanishingly small

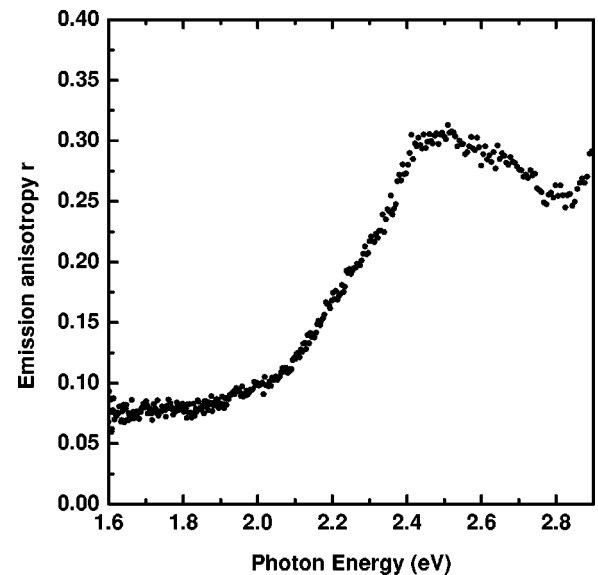


FIG. 6. Anisotropy r in the photoluminescence from PEC-PIFTEH films as a function of photon energy.

degree of polarization is to be expected for the acceptor emission, so that the observed anisotropy in the red part of the PL spectrum (1.6 eV) can be attributed to the partly polarized emission from PIFTEH aggregates. For the calculations we first set a specific value for the relative acceptor concentration $X = \frac{1}{2} \sqrt{\pi} (c_A/c_0)$. We then took a set of random orientations \vec{d}_i , \vec{a}_i , and \vec{r}_i in 3D to describe a randomly oriented donor-acceptor set and calculated its orientation factor κ_i^2 according to Eq. (3). Since $X \propto R_0^3 \propto \sqrt{\kappa^2}$, the parameter X_i upon which the Förster transfer for this particular set depends, can be expressed as

$$X_i = X \frac{\sqrt{\kappa_i^2}}{\langle \sqrt{\kappa^2} \rangle}, \quad (10)$$

where $\langle \sqrt{\kappa^2} \rangle = 0.845 \sqrt{2/3}$ is the average value as calculated by Maksimov and Rozman for a donor-acceptor ensemble with random, but fixed orientations.³⁰ The total transfer probability $\hat{\varphi}$ is then given by

$$\hat{\varphi} = \varphi_T(X_i) \times d_{z,i}, \quad (11)$$

where φ_T is the Förster transfer probability as stated in Eq. (8) and $d_{z,i}$ is the probability that the donor has been excited by the linearly polarized light (whose polarization direction was here chosen to be along the z axis). Note that φ_T does not describe the transition probability for a *single* donor-acceptor pair, but for an *ensemble* of donor-acceptor pairs with a spatially random distribution and a specific relative orientation set by \vec{d}_i , \vec{a}_i , and \vec{r}_i . These steps were performed for 10^8 donor-acceptor sets $\{\vec{d}_i, \vec{a}_i, \vec{r}_i\}$ and the total photoluminescence intensity components along the three coordinate axes were calculated by successive summing over the components from the individual sets. From the total PL intensity components, the emission anisotropy r was then determined. The whole calculation was performed for a wide range of relative acceptor concentrations X , the result of which is displayed in Fig. 7. As expected, the emission anisotropy calculated for the donor ensemble is independent of the acceptor concentration and given by the well-known value $r=0.4$ for an isotropic medium subject to excitation with linearly polarized light.⁴⁶ The emission from the acceptor ensemble, however, is partly polarized at low acceptor concentrations with $r \approx 0.016$, but depolarizes with increasing acceptor concentration. This can be understood from the dependence of the total transfer probability φ_T on the acceptor concentration c_A : While φ_T initially increases approximately linearly with c_A , it approaches $\varphi_T \approx 1$ as $c_A \gg c_0$ and the transfer becomes complete. At high relative acceptor concentrations ($X \gg 1$) any change in the orientational parameter κ_i^2 for a particular donor-acceptor orientation will therefore only have a minor effect on the transfer probability and the transfer becomes independent of the relative orientation of the donors and the acceptors. The reverse effect of Förster transfer from an isotropic ensemble of donors to oriented polymeric chains has recently been utilized to construct PL polarizers, whose efficiency relies precisely on this insensitivity of the Förster transfer efficiency to the relative orien-

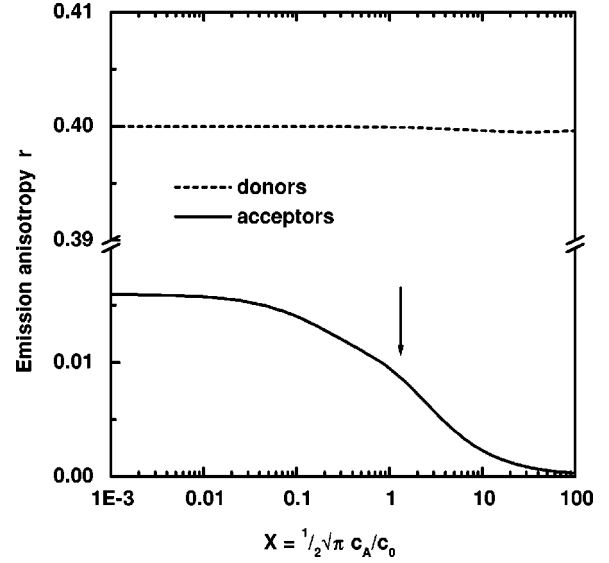


FIG. 7. Emission anisotropy r for a donor and an acceptor ensemble versus relative acceptor concentration X , as calculated using a Monte Carlo simulation (see text). The arrow indicates the relative acceptor concentration for the PEC-PIFTEH samples used in this study.

tation between the donor and the acceptor ensemble at sufficiently high donor concentrations.¹² From our fits to the photoluminescence decay curves, as described above, we extract a value of $X \approx 1.3$ for our system, which yields an expected anisotropy $r = 0.0087$ for the emission from perylene according to the Monte Carlo calculation. Moreover, as the emission anisotropy observed experimentally from the PIFTEH main chain is already below its ideal value ($r = 0.31 < 0.40$), an even lower value for the perylene emission anisotropy is to be expected. Since the observed emission anisotropy in the red spectral region is more than an order of magnitude higher than expected, it can be assumed to be caused almost solely by the emission from PIFTEH aggregates. We can thus estimate the contribution of the aggregate emission to the total emission in the red to be 40% from Eq. (9) by taking the difference spectrum $I_{\parallel} - I_{\perp}$ and assuming $r = 0.31$ for the aggregate emission. Taking the contribution from the aggregate emission into account we can now calculate the ratio $q = \phi_D / \phi_A$ between the number of photons emitted from isolated PIFTEH chains and the number of photons emitted from perylene chains, by integrating over the different spectral contributions to the total PL spectrum $I_{\parallel} + 2I_{\perp}$. We obtain a value of $q = 0.084 \pm 0.008$ and from Eqs. (8) and (5) we extract a Förster radius $R_0 = (1.8 \pm 0.3)$ nm using $\eta_A = 0.74 \pm 0.27$ and $\eta_D = 0.36 \pm 0.04$. This value is in excellent agreement with the Förster radius taken from the time-resolved PL measurements, which suggests that an accurate determination of R_0 is possible from time-integrated photoluminescence measurements, provided that the spectra are taken for both polarization orientations (I_{\parallel} and I_{\perp}).

In the final part of this paper we will calculate the Förster radius from the spectral overlap between the donor emission and the acceptor absorption, using Eq. (2). To calculate the

overlap integral, we have measured the extinction coefficient spectrum ϵ_A for a chloroform solution of a (nonconjugated) polymer consisting of perylene monomers closely related to the perylene derivative used as end caps in PEC-PIFTEH (see Fig. 1). In the red/green spectral region this was found to resemble closely the absorption spectrum of the perylene molecules within PEC-PIFTEH. However, in the blue spectral region (≥ 2.8 eV) the strong absorption from the PIFTEH main chains obscured the absorption from the perylene molecules in PEC-PIFTEH (see inset in Fig. 1). As R_0 is proportional to the sixth root of the overlap integral, even larger variations in the shape of the absorption spectrum would only have a small effect on the value of R_0 , so that the use of the polyperylene absorption spectrum appeared to be a suitable choice. Since we wish to calculate the Förster radius for the excitation transfer to perylene molecules both from isolated PIFTEH chains and from PIFTEH aggregates, we need to calculate the overlap integral of the perylene absorption with the excitonic PIFTEH emission as well as with the aggregate emission. To obtain the solely excitonic luminescence spectrum, we have measured a photoluminescence up conversion spectrum from a pure PIFTEH film at 4 ps after excitation, where the emission is dominated by the recombination of excitons located on isolated PIFTEH chains. For the emission spectrum of the PIFTEH aggregates we have taken the low energy end (1.6–2.4 eV) of the time-integrated PL difference spectrum ($I_{\parallel} - I_{\perp}$) from the PEC-PIFTEH film (Fig. 3, bottom) since it is dominated by the emission from PIFTEH aggregates. Taking $n = 1.9$ (at 2.7 eV) and $n = 1.7$ (at 2.2 eV) as the refractive indices of the PIFTEH film at the peak of the overlap integrals (from ellipsometry), and $\kappa^2 = (0.845\sqrt{2/3})^2$ from Refs. 30, we obtain $R_0(\text{exc}) = \eta_{\text{exc}}^{1/6} \times (3.3 \pm 0.2)$ nm and $R_0(\text{aggr}) = \eta_{\text{aggr}}^{1/6} \times (3.9 \pm 0.2)$ nm for the Förster transfer from isolated PIFTEH chains and from PIFTEH aggregates to perylene molecules, with η_{exc} and η_{aggr} being the quantum efficiencies of the isolated PIFTEH chains and the PIFTEH aggregates. The lowest possible value for η_{aggr} can be estimated from the quantum efficiency of the PEC-PIFTEH film $\eta_{(\text{PEC-PIFTEH})} = 0.47$ and the fraction of the total photons emitted from isolated PIFTEH chains (0.048), from PIFTEH aggregates (0.382), and from the perylene molecules (0.57). For the extreme case that the emission efficiency from both the isolated PIFTEH chains and the perylene molecules is equal to 1, a minimum efficiency of $\eta_{\text{aggr}} = 0.25$ is calculated. This value is not much lower than the quantum efficiency of pure PIFTEH films ($\eta_{(\text{PIFTEH})} = 0.36$) and is consistent with quantum efficiency measurements on different polyindenofluorene films with large variations of the relative contributions from aggregates to the emission; they only show relatively small variations in their quantum efficiencies indicating that the radiative efficiencies for recombination from isolated chains and from PIFTEH aggregates do not vary strongly.⁴⁷ Assuming the ranges $0.36 \leq \eta_{\text{exc}} \leq 1$ and $0.25 \leq \eta_{\text{aggr}} \leq 1$ we can estimate the possible range within which the Förster radius R_0 must fall for the two types of transfer. The results are given in Table I together with the experimental values determined from the photoluminescence measurements. As can be seen, the values determined from the experimental PL data are

TABLE I. Förster radii for transfer of excitations located on isolated PIFTEH chains [$R_0(\text{exc})$] and those at PIFTEH aggregate sites [$R_0(\text{aggr})$] to perylene molecules, taken from photoluminescence measurements as well as from spectral overlap calculations

	from PL measurements	from spectral overlap
$R_0(\text{exc})(\text{nm})$	1.8 ± 0.3	2.8–3.3
$R_0(\text{aggr})(\text{nm})$	negligible	3.1–3.9

significantly lower than those expected from spectral overlap calculations, especially for the excitation transfer from PIFTEH aggregate sites to perylene molecules where a value of $R_0 \approx 3.5$ nm is predicted from spectral overlap calculations, but no transfer is actually observed. These discrepancies can be explained if the sample morphology is taken into account: within regions of the PEC-PIFTEH film where interchain interactions are strong, the PIFTEH chains will be closely packed and ordered to some extent,⁴⁸ so that there will be a reduced possibility for perylene molecules to be found in close proximity to a PIFTEH chain. As the Förster transfer rate is strongly dependent on the donor-acceptor separation, the transfer efficiency from aggregate states to perylene acceptors is reduced substantially. A similar, but weaker effect will influence the transfer of excitation from isolated PIFTEH chains: because the excitation is located on a long indenofluorene chain, part of its surrounding volume is taken up by two continuing ends of the chain and is therefore less likely to be occupied by a perylene molecule. We conclude that the assumption of a spatially random distribution of donors and acceptors, which enters in the derivation of the Förster transfer rate given in Eq. (4), is not always applicable to a polymeric guest-host system, especially when aggregation is likely to occur within the sample. Migration of excitations within the sample may compensate for some of these effects and increase the Förster transfer efficiency,⁵ however, this mechanism may prove less effective for Förster transfer from aggregate sites where the diffusivity of excitations is often limited.³⁴

IV. CONCLUSION

We have studied the excitation transfer in a novel polymer/dye system consisting of thin films of polyindenofluorene chains as the host and perylene molecules covalently bonded to the chain ends as the guests. We have extracted the Förster radius R_0 for transfer of excitons from isolated PIFTEH chains to perylene endcaps to be (1.8 ± 0.3) nm. The emission anisotropy for both donors and acceptors was modelled via a Monte Carlo simulation based on Förster theory; the results confirm that for the case of efficient transfer the acceptor is expected to emit unpolarized light. It was shown that a reliable value for the Förster radius can therefore be extracted from simple time-integrated PL measurements, as the donor and the acceptor contribution to the emission can be spectrally separated if PL spectra are taken for polarization orientations both parallel and perpendicular to the excitation direction. Finally, we have found that while a large efficiency is expected for the transfer of excitations

form PIFTEH aggregates to perylene molecules from spectral overlap calculations, no transfer is actually observed. We attribute this to chain packing effects within the sample prohibiting sufficiently close contact between the PIFTEH aggregates and the perylene molecules. Our findings are important for the design of LEDs and lasers based on polymeric guest-host systems as the active layer: due to the absence of excitation transfer from aggregate sites, the emission from these sample regions forms a constant background in the luminescence thereby limiting the tunability of the emission color with changes in the acceptor concentration. Moreover, the inhomogeneous distribution of the aggregate states, as well as their often comparatively small transition dipole moment will increase the threshold for amplified spontaneous

emission to occur in their spectral region. Host aggregation in polymeric guest-host systems is therefore undesirable for both LEDs and lasers and should best be avoided, e.g., through choice of suitable chain side groups or processing techniques.

ACKNOWLEDGMENTS

We would like to thank C.M. Lynn for the refractive index measurements and J.D. Mackenzie for providing the luminescence efficiency data for the polymer films. This work was supported by the European Commission (TMR program “Ultrafast Quantum Optoelectronics” and BRITE EURAM Contract No. BRPR-CT97-0469, “OSCA”).

- ¹R.H. Friend, R.W. Gymer, A.B. Holmes, J.H. Burroughes, R.N. Marks, C. Taliani, D.D.C. Bradley, D.A.D. Santos, J.L. Brédas, M. Lögdlund, and W.R. Salaneck, *Nature (London)* **397**, 121 (1999).
- ²T. Virgili, D.G. Lidzey, and D.D.C. Bradley, *Adv. Mater.* **12**, 58 (2000).
- ³S. Tasch, E.J.W. List, C. Hochfilzer, G. Leising, P. Schlichting, U. Rohr, Y. Geerts, U. Scherf, and K. Müllen, *Phys. Rev. B* **56**, 4479 (1997).
- ⁴G. Cerullo, M. Nisoli, S. Stagira, S.D. Silvestri, G. Lanzani, W. Graupner, E. List, and G. Leising, *Chem. Phys. Lett.* **288**, 561 (1998).
- ⁵E.J.W. List, C. Creely, G. Leising, N. Schulte, A.D. Schlüter, U. Scherf, K. Müllen, and W. Graupner, *Chem. Phys. Lett.* **325**, 132 (2000).
- ⁶A. Dogariu, R. Gupta, A.J. Heeger, and H. Wang, *Synth. Met.* **100**, 95 (1999).
- ⁷R. Gupta, M. Stevenson, M.D. McGehee, A. Dogariu, V. Srdanov, J.Y. Park, and A.J. Heeger, *Synth. Met.* **102**, 875 (1999).
- ⁸M. Berggren, A. Dodabalapur, R.E. Slusher, and Z. Bao, *Synth. Met.* **91**, 65 (1997).
- ⁹E.J.W. List, L. Holzer, S. Tasch, G. Leising, U. Scherf, K. Müllen, M. Catellani, and S. Luzzati, *Solid State Commun.* **109**, 455 (1999).
- ¹⁰M.D. McGehee, T. Bergstedt, C. Zhang, A.P. Saab, M.B. O'Regan, G.C. Bazan, V.I. Srdanov, and A.J. Heeger, *Adv. Mater.* **11**, 1349 (1999).
- ¹¹S. Tasch, E.J.W. List, O. Ekström, W. Graupner, G. Leising, P. Schlichting, U. Rohr, Y. Geerts, U. Scherf, and K. Müllen, *Appl. Phys. Lett.* **71**, 2883 (1997).
- ¹²A. Montali, C. Bastiaansen, P. Smith, and C. Weder, *Nature (London)* **392**, 261 (1998).
- ¹³A. Montali, G.S. Harms, A. Renn, C. Weder, P. Smith, and U.P. Wild, *Phys. Chem. Chem. Phys.* **1**, 5697 (1999).
- ¹⁴L. Chen, L.S. Roman, D.M. Johansson, M. Svensson, M.R. Andersson, R.A.J. Janssen, and O. Inganäs, *Adv. Mater.* **12**, 1110 (2000).
- ¹⁵P. Haring Bolivar, G. Wegmann, R. Kersting, M. Deussen, U. Lemmer, R.F. Mahrt, H. Bässler, E.O. Göbel, and H. Kurz, *Chem. Phys. Lett.* **245**, 534 (1995).
- ¹⁶D. Marsitzky, S. Becker, S. Setayesh, K. Müllen, J. D. Mackenzie, and R. H. Friend (unpublished).
- ¹⁷S. Setayesh, D. Marsitzky, and K. Müllen, *Macromolecules* **33**, 2016 (2000).
- ¹⁸T. Förster, *Ann. Phys. (Leipzig)* **2**, 55 (1948).
- ¹⁹T. Förster, *Naturwissenschaften* **33**, 166 (1946).
- ²⁰W.L. Lewschin, *Z. Phys.* **26**, 274 (1924).
- ²¹F. Weigert and G. Käßler, *Z. Phys.* **25**, 99 (1924).
- ²²E. Gaviola and P. Pringsheim, *Z. Phys.* **24**, 24 (1924).
- ²³T. Förster, *Fluoreszenz Organischer Verbindungen* (Vandenhoeck and Ruprecht, Göttingen, 1951).
- ²⁴T. Förster, *Discuss. Faraday Soc.* **27**, 7 (1959).
- ²⁵T. Förster, in *Modern Quantum Chemistry*, edited by O. Sinanoglu (Academic Press, London, 1965).
- ²⁶D.L. Dexter, *J. Chem. Phys.* **21**, 836 (1953).
- ²⁷Note that this equation has been printed incorrectly with π^6 instead of π^5 in Refs. 23 and 24, as pointed out by Förster in Ref. 25, p. 135 (footnote). Unfortunately, this error has been transferred to some recently published articles (Ref. 6).
- ²⁸R.C. Powell and Z.G. Soos, *J. Lumin.* **11**, 1 (1975).
- ²⁹K.B. Eisenthal and S. Siegel, *J. Chem. Phys.* **41**, 652 (1964).
- ³⁰M.Z. Maksimov and I.M. Rozman, *Opt. Spectrosc.* **12**, 337 (1961).
- ³¹T. Förster, *Z. Naturforsch. A* **4**, 321 (1949).
- ³²R.C. Powell, *Phys. Rev. B* **2**, 2090 (1970).
- ³³R.C. Powell and R.G. Kepler, *Phys. Rev. Lett.* **22**, 636 (1969).
- ³⁴L.M. Herz and R.T. Phillips, *Phys. Rev. B* **61**, 13691 (2000).
- ³⁵C. Silva, D.M. Russel, M.A. Stevens, J.D. Mackenzie, S. Setayesh, K. Müllen, and R. Friend, *Chem. Phys. Lett.* **319**, 494 (2000).
- ³⁶L.M. Herz, C. Silva, R. T. Phillips, S. Setayesh, and K. Müllen, *Chem. Phys. Lett.* (to be published).
- ³⁷V.N. Bliznyuk, S.A. Carter, J.C. Scott, G. Klärner, R.D. Miller, and D.C. Miller, *Mater. Charact.* **32**, 361 (1999).
- ³⁸J.B. Birks, *Rep. Prog. Phys.* **38**, 903 (1975).
- ³⁹R.S. Knox, *Physica (Amsterdam)* **39**, 361 (1968).
- ⁴⁰E.L. Eriksen and A. Ore, *Phys. Norv.* **2**, 159 (1967).
- ⁴¹I.D.W. Samuel, G. Rumbles, and C.J. Collison, *Phys. Rev. B* **52**, R11 573 (1995).
- ⁴²R.F. Mahrt, T. Pauck, U. Lemmer, U. Siegner, M. Hopmeier, R. Hennig, H. Bässler, E.O. Göbel, P.H. Bolivar, G. Wegmann, H. Kurz, U. Scherf, and K. Müllen, *Phys. Rev. B* **54**, 1759 (1996).

- ⁴³C. Silva, L.M. Herz, D. Russel, D. Mackenzie, S. Setayesh, K. Müllen, R.T. Phillips, R.H. Friend, D. Beljonne, G. Pourtois, and J.-L. Bredas (unpublished).
- ⁴⁴R. Kersting, U. Lemmer, R.F. Mahrt, K. Leo, H. Kurz, H. Bässler, and E.O. Göbel, *Phys. Rev. Lett.* **70**, 3820 (1993).
- ⁴⁵B. Mollay, U. Lemmer, R. Kersting, R.F. Mahrt, H. Kurz, H.F. Kauffmann, and H. Bässler, *Phys. Rev. B* **50**, 10 769 (1994).
- ⁴⁶F. Perrin, *Ann. Phys. (Leipzig)* **12**, 169 (1929).
- ⁴⁷J.D. Mackenzie (private communication).
- ⁴⁸J.W. Blatchford, T.L. Gustafson, A.J. Epstein, D.A.V. Bout, J. Kerimo, D.A. Higgins, P.F. Barbara, D.K. Fu, T.M. Swager, and A.G. MacDiarmid, *Phys. Rev. B* **54**, R3683 (1996).